E-396

FERMILAB-CONF-82-110-E

Rockefeller University
Report No. DOE/ER/40033-33

(RU 81/A-32)

DIFFRACTIVE JETS

K. Goulianos

The Rockefeller University, New York, NY 10021 USA

Presented at

Europhysics Study Conference
Jet Structure from Quark and Lepton Interactions

Erice-Trapani-Sicily
12-17 September 1982

FERMILAB

NOV 11 1982

LIBRARY

DIFFRACTIVE JETS

K. Goulianos

The Rockefeller University
New York, NY 10021 USA

We review the properties of particle clusters produced in the processes of single and double diffraction dissociation of protons at high energies:

$$p + p \to X + p$$
$$\quad\quad \hookrightarrow n_c + \text{neutrals} \tag{1}$$

$$p + p \to X_1 + X_2 \tag{2}$$

These clusters appear as jets close to the direction of the dissociating protons and henceforth will be referred to as diffractive or forward jets.

Our review is organized as follows: After a brief introduction into the phenomenology of diffraction dissociation, we discuss the production cross sections of the diffractive states X, their multiplicity distributions, and the angular or pseudorapidity distributions of the dissociation products. Throughout our discussion we emphasize the points that allow one to predict the properties of diffractive jets at the SPS and Fermilab $\bar{p}p$ Colliders ($\sqrt{s}$ = 540 and 2000 GeV, respectively).

I. PHENOMENOLOGY OF DIFFRACTION DISSOCIATION

The amplitude for single diffraction dissociation is presented schematically in Figure 1.

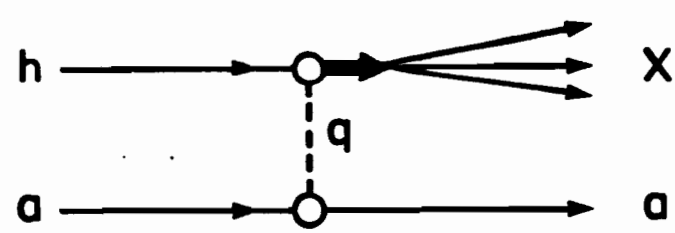

Fig. 1. Amplitude for diffraction dissociation of a hadron h on a target particle a (schematic).

The excitation mass, M_x, is related to the forward component of the four-momentum transfer, $q_{\parallel}$, and to the Feynmann x variable, $x = p^*_{\parallel}/p^*_{\parallel,max}$ of the recoil proton, as follows:

$$|q_{\parallel}| = m_p \frac{M_x^2 - M_h^2}{s} \cong m_p(1-x) \tag{3}$$

As the wave length associated with $q_{\parallel}$, $\lambda = 1/|q_{\parallel}|$, becomes larger than the interaction radius, $R \cong 1/m_{\pi}$, one expects coherence or diffraction phenomena to appear. Thus, the condition for inelastic diffraction is

$$1/|q_{\parallel}| \gtrsim R \cong \frac{1}{m_{\pi}} \tag{4a}$$

$$1 - x \cong \frac{M_x^2 - M_h^2}{s} \lesssim \frac{m_{\pi}}{m_p} \cong 0.15 \tag{4b}$$

As seen in Figure 2, the differential cross section, $d^2\sigma/dtdx$, which is fairly flat in the central x region (not shown entirely in the figure), increases rapidly with decreasing 1-x in the region $1-x \lesssim 0.15$.

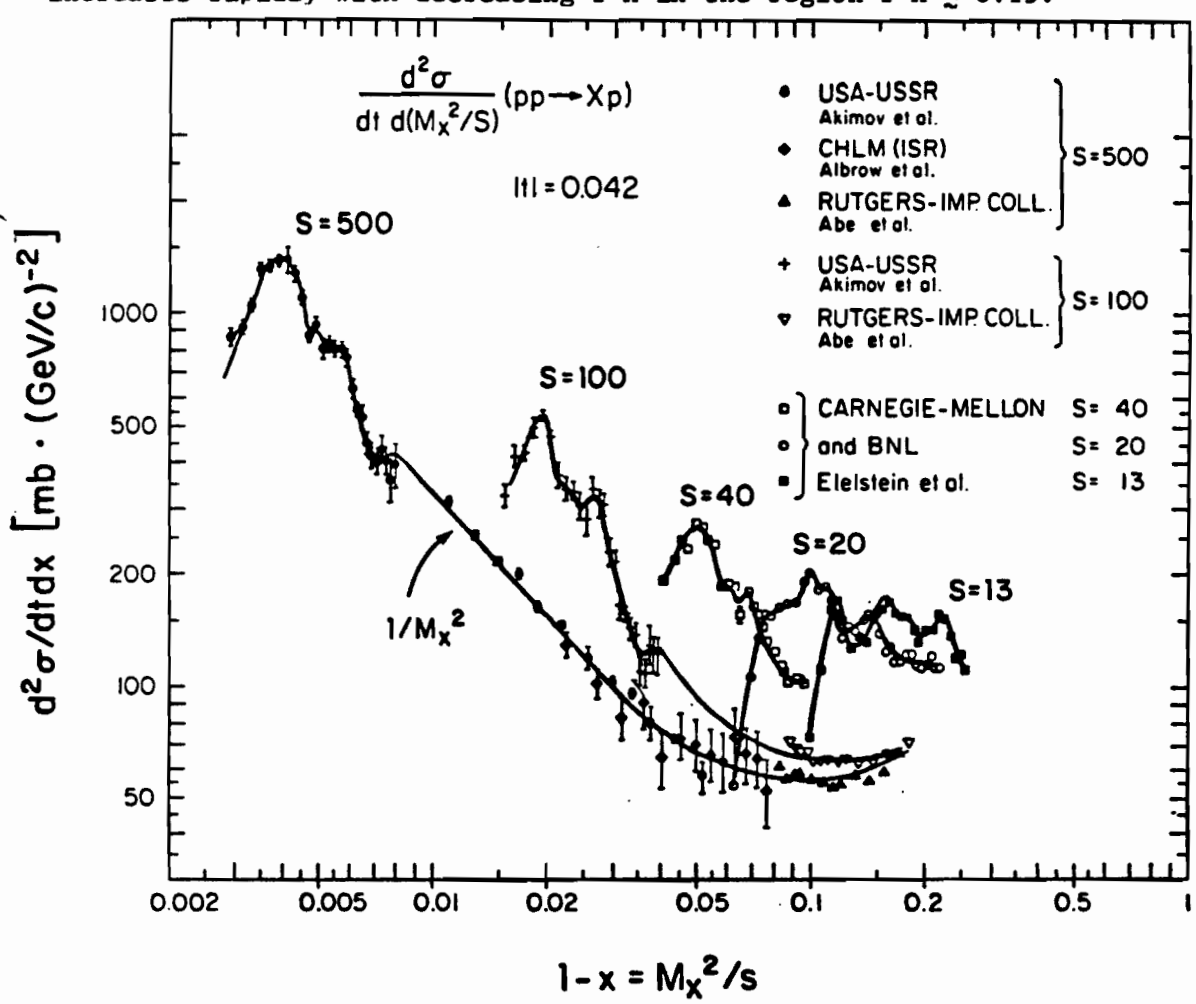

Fig. 2. The inclusive single diffraction dissociation cross section $d^2\sigma/dtdx$ versus 1-x for $pp \to Xp$ at various values of s. As the energy increases, the low mass "resonance region" moves to smaller values of 1-x while larger masses enter the diffraction region to form a $1/M_x^2$ continuum [from K. Goulianos, Proc. XIIIth Rencontre de Moriond, Vol. I (1978), pp. 457-459].

This increase is attributed to the setting in of the coherence condition and, therefore, the peak at small 1-x is identified as "diffractive." The higher the s-value, the larger the M_x^2 that fulfills the ocherence condition. At the Fermilab $\bar{p}p$ Collider, $\sqrt{s}$ = 2000 GeV, the mass corresponding to $M_x^2/s = 0.15$ is M_x = 780 GeV ! As larger mass states are produced diffractively, the overall diffraction dissociation cross section increases. At $\sqrt{s}$ = 2000 GeV, about one-half of the inelastic cross section is expected to be due to single and double diffraction dissociation.

The differential cross section

$$\frac{d^2\sigma^{ha}}{dtdM_x^2} = f_{h,a}\ (s,t,M_x^2) \tag{4}$$

depends weakly on s, is exponential in t, varies as $1/M_x^2$ and obeys factorization and the finite mass sum rule. This behavior is consistent with the hypothesis that diffraction dissociation is dominated by a triple-Pomeron Regge type amplitude.

The phenomenology of diffraction idssociation is discussed in detail in an article prepared by the author[1] for publication in Physics Reports. In the next three sections we review the properties of diffraction dissociation which are relevant to the understanding of diffractive jets.

II. DIFFRACTION DISSOCIATION CROSS SECTIONS

We discuss separately the single and double diffraction dissociation cross sections:

A. Single Diffraction Dissociation Cross Section

The differential cross section for single diffraction dissociation of protons on protons is given by[1]

$$\frac{d^2\sigma}{dtdM_x^2} = \frac{A}{M_x^2}\left(1 + \frac{B}{s}\right)\ \left(b_{SD}\ e^{b_{SD}t}\right) \tag{5}$$

where A = 0.68 ± 0.05 mb, B = 36 ± 8 GeV^2 and $b_{SD}/b_{e\ell} \cong 2/3$ to 1/2. At Fermilab and ISR energies, the slope for single diffraction dissociation is $b_{SD} \cong 7\ (\mathrm{GeV/c})^{-2}$. The average $|t|$ of the diffractive states is thus $1/b_{SD} \cong 0.14\ (\mathrm{GeV/c})^2$, corresponding to $p_T \cong 380$ MeV/c. At a beam momentum of 30 GeV/c (ISR), the diffractive states are produced at an average angle of $\sim$13 mrad. At the Fermilab Collider, the average production angle will be $\sim$0.3 mrad. Thus, the characterization of the particle clusters arising from the dissociation of these states as "forward" jets is justified.

Integrating the differential cross section over t and M_x^2 (from M_x^2 = 1 GeV^2 to 0.1s) yields the total single diffraction dissociation cross section

$$\sigma_{SD} = 0.68\ \ell n(0.1s)\ \mathrm{mb} \tag{6}$$

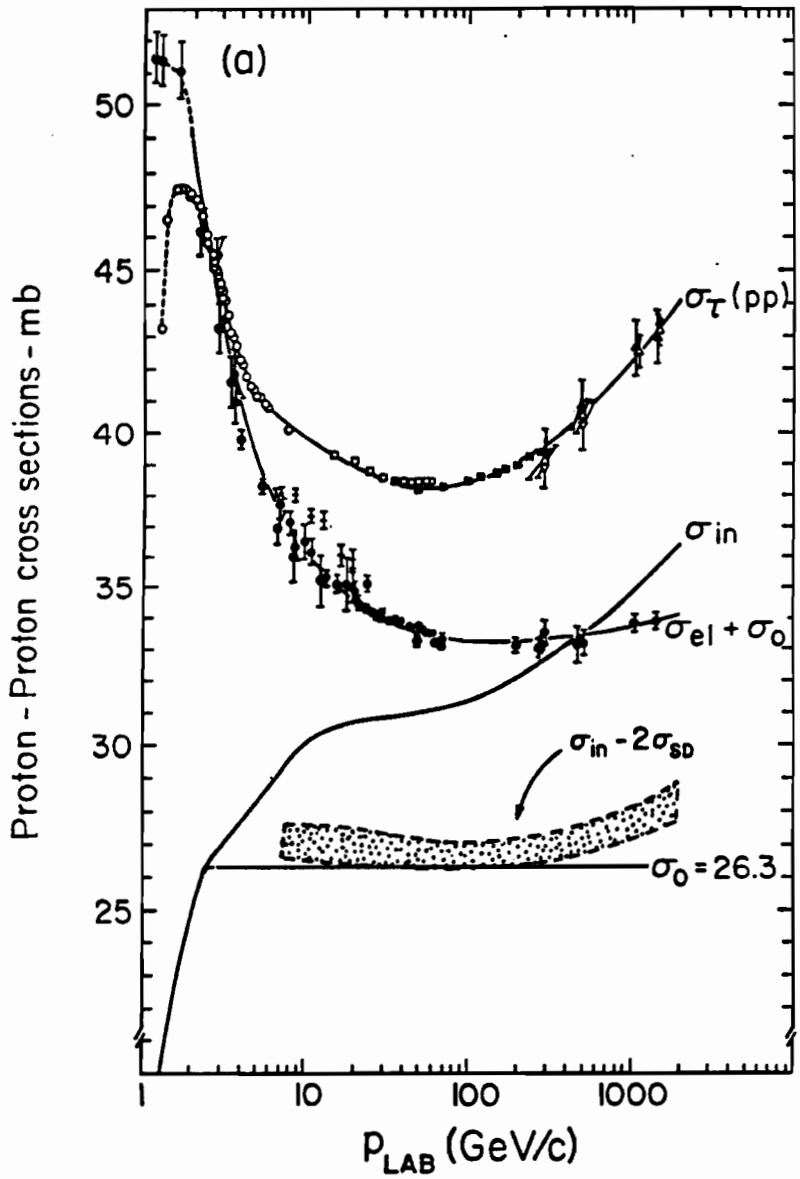

Fig. 3. Proton-proton cross sections as a function of laboratory momentum. After subtraction of twice the single diffraction dissociation cross section, as given by Eq. (6), the remaining rise of the inelastic cross section with energy is small and consistent with the expected contribution from double diffraction dissociation (see text).

Figure 3 shows σ_T, $\sigma_{e\ell}$, σ_{in} and $\sigma_{in} - 2\sigma_{SD}$ for pp interactions. The total and elastic cross sections have been fitted empirically[2]. The inelastic cross section is obtained by subtracting the elastic from the total. Further subtraction of twice the single diffraction dissociation cross section from σ_{in} (each one of the two protons can dissociate) yields a cross section which is fairly flat with energy over the entire range from 2 to 2000 GeV. As will be shown in Section B below, the remaining rise of $\sigma_{in} - 2\sigma_{SD}$ with energy is consistent with being due to double diffraction dissociation. Thus, the non-diffractive "hard core" of the pp cross section appears to be flat with energy and one may write the total cross section as

$$\sigma_T = \sigma_o + \sigma_{e\ell} + 2\sigma_{SD} + \sigma_{DD} \tag{7}$$

where $\sigma_o = 26.3$ mb and σ_{DD} is the cross section for double diffraction dissociation.

B. Double Diffraction Dissociation Cross Section

The differential cross section for double diffraction dissociation may be obtained from the cross sections for single diffraction dissociation and elastic scattering using factorization:

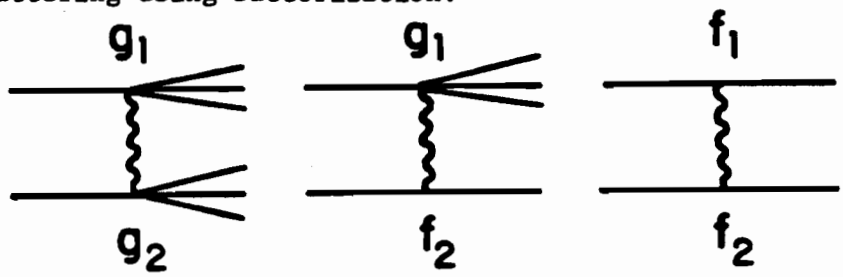

$$(g_1 g_2)^2 = \frac{(g_1 f_2)^2 \quad (f_1 g_2)^2}{(f_1 f_2)^2}$$

$$\frac{d^3\sigma}{dt dM_1{}^2 dM_2{}^2} = \frac{d^2\sigma_1}{dt dM_1{}^2} \; \frac{d^2\sigma_2}{dt dM_2{}^2} \Big/ \frac{d\sigma_{e\ell}}{dt} \tag{8}$$

Assuming e^{bt} dependence for both single diffraction dissociation and elastic scattering, integration of Eq. (8) yields

$$\sigma_{DD} = k \frac{\sigma_{SD}{}^2}{\sigma_{e\ell}} \; ; \quad k = \frac{r^2}{2r-1} \; ; \quad r = \frac{b_{SD}}{b_{e\ell}} \tag{9}$$

For $r = 2/3$, $k = 4/3$ while for $r = 1/2$, $k = \infty$. Because of the sensitivity of the coefficient k on the value of r, the calculation of σ_{DD} using Eq. (9) has a large uncertainty. Since experimentally $r \lesssim 2/3$, a lower bound for σ_{DD} may be obtained by using $r = 2/3$ or $k = 4/3$. At 200 and 2000 GeV/c, this yields $\sigma_{DD} \cong 1.4$ and 2.8 mb, respectively, corresponding to a rise of 1.4 mb between the two energies. This is close to the rise represented by the dotted band in Figure 3, consistent with an energy independent hard core.

The double diffraction dissociation cross section may also be obtained from Eq. (7): $\sigma_{DD} = \sigma_T - \sigma_o - \sigma_{e\ell} - 2\sigma_{SD}$. Since the hard core may increase with energy, using $\sigma_o = 26.3$ mb gives an upper bound for σ_{DD}. As examples, we calculated σ_{DD} for the SPS and Fermilab $\bar{p}p$ Colliders. We take $\sigma_T = 57$ and 64 mb at $\sqrt{s} = 540$ and 2000 GeV, respectively, as predicted by the critical Pomeron reggeon field theory[3]. Then

	$\sqrt{s} = 540$	$\sqrt{s} = 2000$
σ_T	57.0 mb	64.0 mb
σ_o	26.3	26.3
$\sigma_{e\ell} = 0.175\ \sigma_T$	10.0	11.2
$\sigma_{SD} = 0.68\ \ell n\ (0.1s)$	7.0	8.8
$\sigma_{DD} = \sigma_T - \sigma_o - \sigma_{e\ell} - 2\sigma_{SD}$	6.7	8.9
$\sigma_{DD} = 4/3\ \frac{\sigma_{SD}{}^2}{\sigma_{e\ell}}$	6.5	9.2

Although the two methods of calculating σ_{DD} are in good agreement, we emphasize that they are both subject to uncertainties. Only a measurement of σ_{DD}, along with $\sigma_{e\ell}$ and σ_{SD}, can yield the coefficient k of Eq. (9) and, given σ_T, check the validity of Eq. (7). Such a measurement has been proposed for the Fermilab Collider[4].

III. DIFFRACTIVE CHARGED MULTIPLICITY DISTRIBUTION

The charged multiplicity distribution of high mass diffractive $\pi^{\pm}$, $K^{\pm}$ and $p^{\pm}$ states is represented well[5,6] by a simple Gaussian function that depends only on the available mass $M \cong M_x - M_h$, peaks at $n_o \cong 2M^{\frac{1}{2}}$, where M is in GeV, and has a peak to width ratio $n_o/D \cong 2$:

$$P_n = \frac{\sigma_n}{\sigma} = \frac{2}{\sqrt{2\pi}\, D} \exp -\left[\frac{(n-n_o)^2}{2D^2}\right] \tag{10}$$

$$n_o \cong 2M^{\frac{1}{2}} \qquad \text{(M in GeV)}$$

$$n_o/D \cong 2$$

The normalization is such that at any value of M the sum of P_n over odd values of n is unity (to within $\sim 1\%$).

Figures 4 and 5 show fits of Eq. (10) to data. In calculating values of $\langle n \rangle$ and D to compare with the data, one must sum over the physical positive values of n only. This shifts the average by $\sim 4\%$ above the value of n_o and the width down by $\sim 6\%$, so that the average multiplicity is $\langle n \rangle = 2.08\, M^{\frac{1}{2}}$ and the $\langle n \rangle/D$ ratio is 2.2, in agreement with the data.

The form (10) of the probability distribution implies that KNO-scaling is satisfied; i.e., the product $P_n \cdot \langle n \rangle$ is a function of $n/\langle n \rangle$ only and not a function of n. Indeed, Eq. (10) may be rewritten as

$$P_n \cdot n_o = \left(\frac{8}{\pi}\right)^{\frac{1}{2}} e^{-2(1-n/n_o)^2} \tag{11}$$

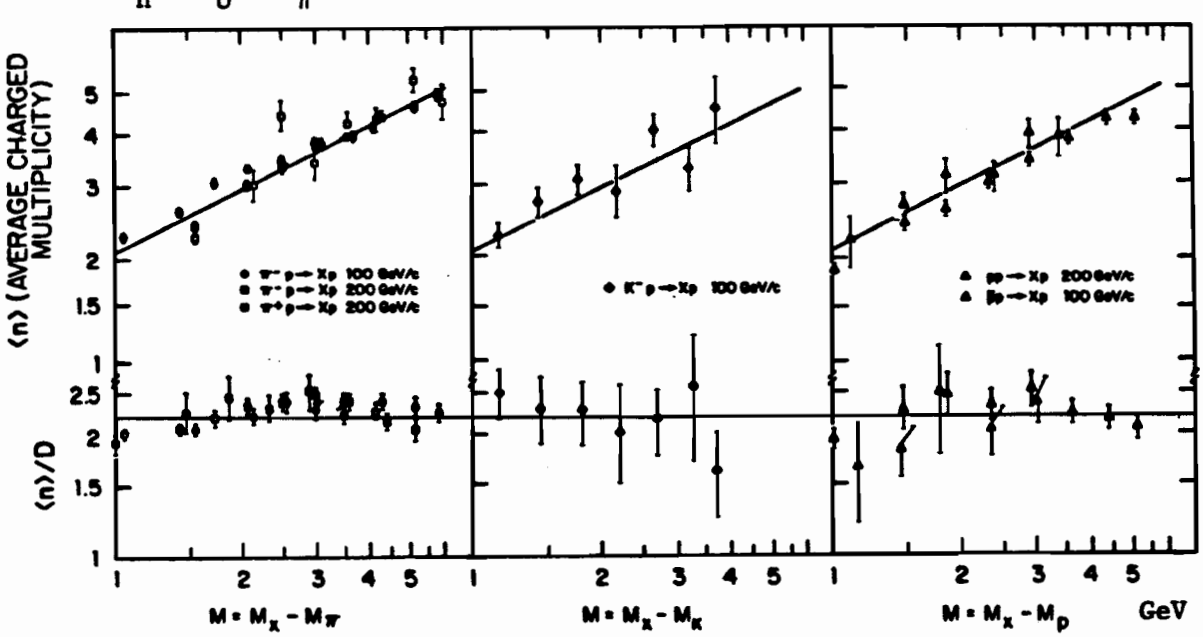

Fig. 4. Average charged multiplicity and ratio of average to width as a function of available mass for $hp \to Xp$ ($h = \pi^{\pm}, K^{\pm}, p^{\pm}$) [Refs. 5,6].

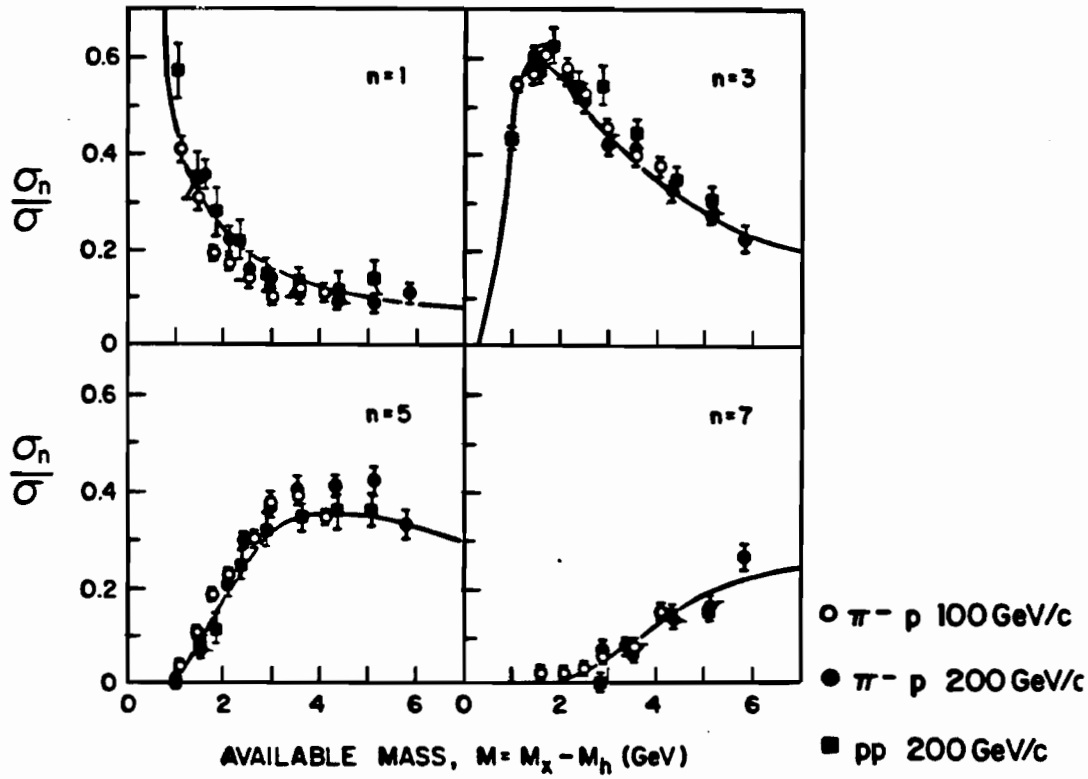

Fig. 5. Charged multiplicity fractions versus available mass for diffractive states X produced in pp → Xp and $\pi^- p \to Xp$ [Refs. 5 and 6].

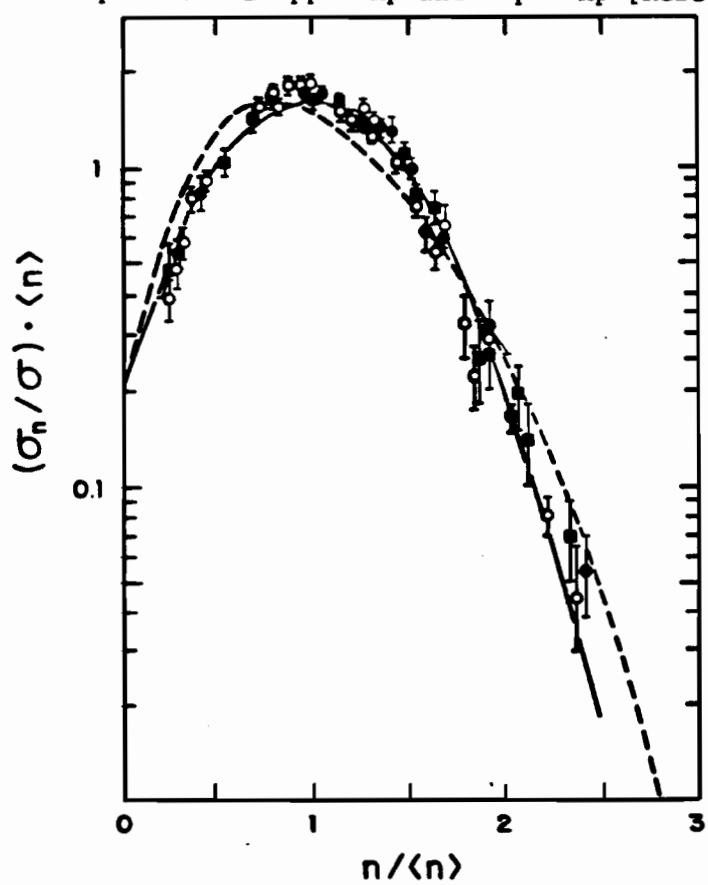

Fig. 6. KNO-scaling distribution for the data presented in Fig. 5. The solid line represents the Gaussian function discussed in the text (Eq. 11). The broken line is from a fit to the inclusive data hp → anything ($h=p,\pi^-$) [Refs. 5 and 6].

Figure 6 shows $P_n \cdot \langle n \rangle$ versus $n/\langle n \rangle$ for $\pi^- p$ and pp diffractive data. Ignoring the small difference between $\langle n \rangle$ and n_o, function (11) represents the data well. However, one observes that in contrast to the fully inclusive reactions $\pi p \rightarrow$ anything and pp $\rightarrow$ anything whose KNO-scaling curve, also shown in Figure 6, is asymmetric and peaks at $n/\langle n \rangle \approx 0.8$, the distribution for the diffractive data is symmetric about the peak at $n/\langle n \rangle = 1$.

For pp $\rightarrow$ anything, the average multiplicity is smaller than $2(\sqrt{s})^{\frac{1}{2}}$ (see Fig. 7a), the $\langle n \rangle/D$ ratio decreases as the energy increases (see Fig. 7b), and the KNO distribution, as mentioned above, is asymmetric about $n/\langle n \rangle = 1$ (see Fig. 8). Nevertheless, Eq. (10) still provides a good description of the data if applied separately to the two distinct sectors of the inelastic cross section: the diffractive component, for which the available mass is $M = M_x - M_p$, and the non-diffractive "hard core" for which $M = \sqrt{s} - 2M_p$. The solid curves in Figures 7 and 8, derived in this manner[6,7], are in excellent agreement with the data.

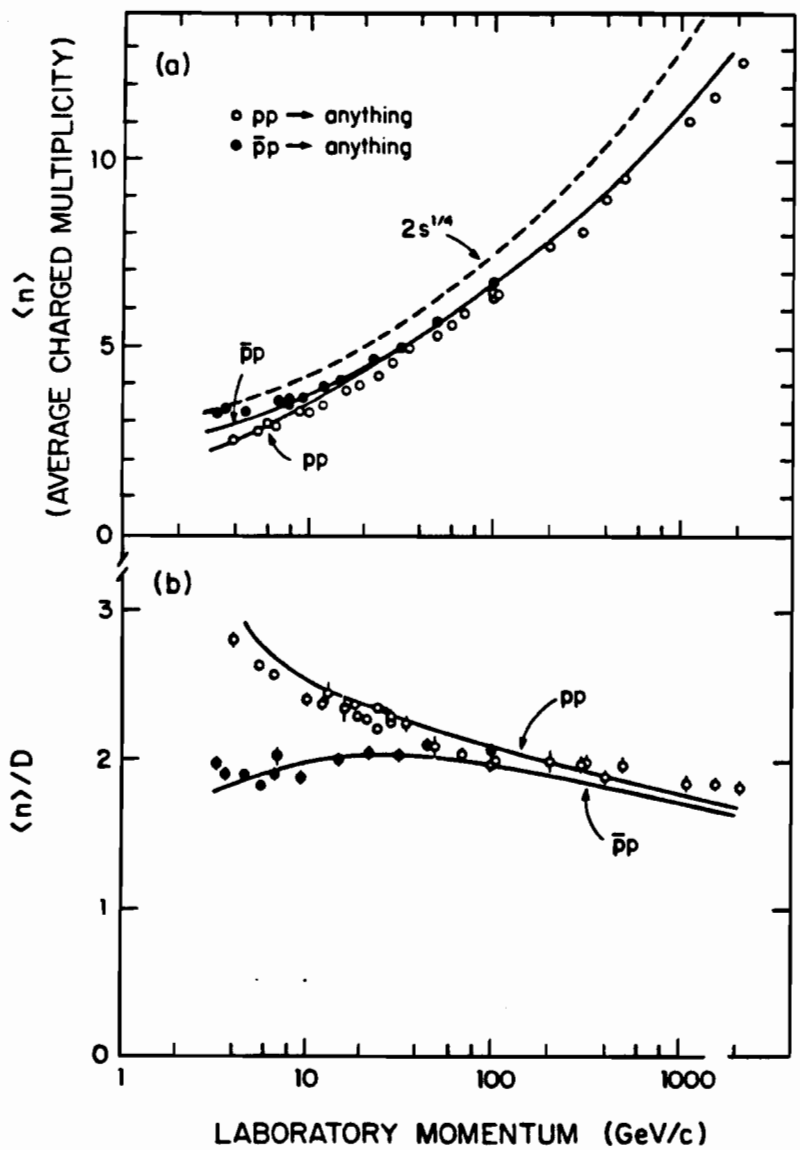

Fig. 7. The average charged multiplicity and the ratio of the average to the width as a function of p_{lab} for pp $\rightarrow$ anything and $\bar{p}p \rightarrow$ anything. The solid curves were calculated using Eq.(10) at the appropriate available mass of the diffractive and non-diffractive components of the inelastic cross section.

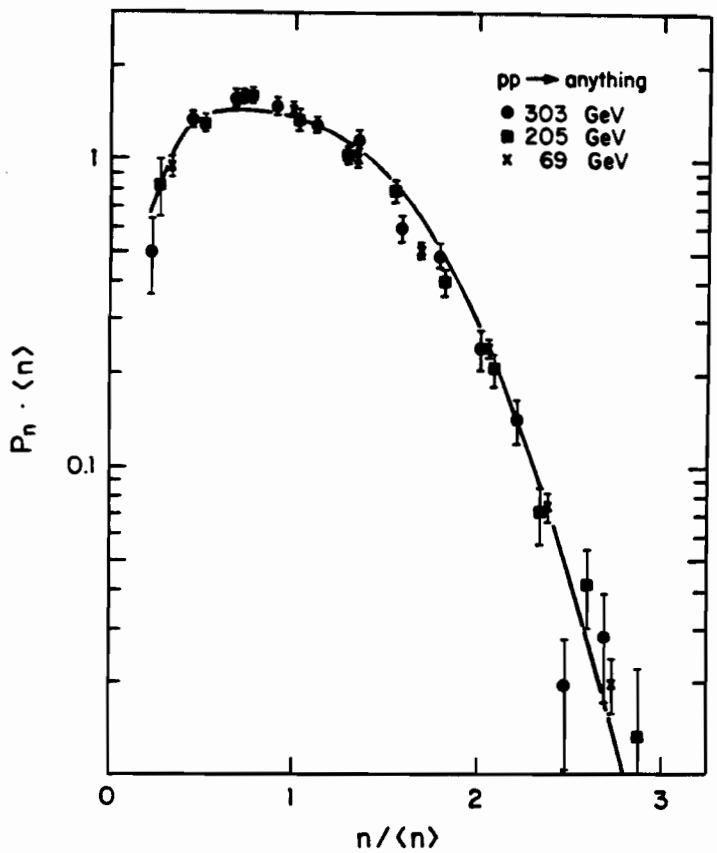

Fig. 8. KNO-scaling distribution for charged particles in pp → anything. The curve was calculated using Eq.(10) separately for the diffractive and non-diffractive components of the inelastic cross section.

An examination of data from several other reactions, including e^+e^- → hadrons, led to the conclusion that the distribution represented by Eq. (10) is universal, describing well all known hadronic charged multiplicities up to and including the highest ISR energies ($\sqrt{s} \cong 60$ GeV). Small differences in the multiplicities between certain reactions, such as between pp and $\bar{p}p$ at the ISR, which cannot be explained by the procedure of applying Eq. (10) at the appropriate available mass of each identifiable component of the inelastic cross section, may then be attributed to the difference in the quark content of the initial states.

IV. DIFFRACTIVE PSEUDO-RAPIDITY DISTRIBUTION

The pseudo-rapidity of a particle produced in the dissociation of a diffractive state X is given by

$$\eta_x = \frac{1}{2} \ln \frac{1 + \cos \theta_x}{1 - \cos \theta_x} \tag{12}$$

where θ_x is the polar angle in the center of mass of the state. The distribution of the charged particles from an isotropic decay of a diffractive state is

$$\frac{dn_c}{d\eta} = \frac{2\, n_c}{(e^{\eta_x} + e^{-\eta_x})^2} \quad ; \quad \eta_x = \eta - \bar{\eta} \tag{13}$$

where n_c is the total number of charged particles in the decay and $\bar{\eta}$ their average pseudo-rapidity given by

$$\bar{\eta} \equiv \eta_M = \frac{1}{2} \ln \frac{s}{M_x^2} \tag{14}$$

The distribution represented by Eq. (13) is plotted in Figure 9. It is very similar to a Gaussian function with a standard deviation

$$\sigma_{\eta_x} \cong \pm 0.7$$

Results[8] from the Pisa-Stony Brook experiment at the ISR (Figs. 10 and 11) show that the pseudo-rapidity distribution for diffractive events of a given multiplicity (corresponding to a given M_x) is consistent with a Gaussian function of width ± 0.6 to ± 1.0, and therefore consistent with Eq. (13). This implies that the diffractive states do indeed decay isotropically. In contrast, non-diffractive events, centered around $\bar{\eta} = 0$, have pseudo-rapidity widths that are much larger than ± 0.7, reflecting the limited transverse momentum behavior of high energy collisions.

Figure 12 shows typical diffractive pseudo-rapidity distributions expected at the Fermilab $\bar{p}p$ Collider ($\sqrt{s}$=2000 GeV) under the assumptions that the average charged multiplicity is given by $n_c = 2\, M_x^{1/2}$ and that the decay is isotropic. Since the cross section for diffraction dissociation is $d\sigma/dM_x^2 = A/M_x^2$ (Eq. 5), it follows from Eq. (14) that $d\sigma/d\eta_M = 2A = 1.36$ mb/ ($\Delta\eta_M = 1$); i.e., the diffractive masses are produced uniformly in rapidity space. Figure 12 then implies that the diffractive charged multiplicities increase as the rapidity decreases. Indeed, integrating over the entire single diffraction dissociation cross section one obtains

$$\left(\frac{dn_c}{d\eta}\right)_{\text{all } M_x^2} = \frac{2s^{1/4}}{\frac{1}{2}\ln s} \quad e^{-\eta/2} \quad e^{b_{SD}\, t_{min}} \tag{15}$$

where the factor $\exp(b_{SD} t_{min})$ imposes a cut-off due to loss of coherence. From Eqs. (3) and (14),

$$t_{min} = -\left[m_p\left(\frac{M_x^2}{s}\right)\right]^2 = -m_p^2 \quad e^{-4\eta_M} \tag{16}$$

The expression in Eq. (15) has, therefore, a maximum at the value of η for which $\eta/2 + b_{SD} m_p^2\, e^{-4\eta}$ is minimum, or at $\eta = 1/4 \ln (8m_p^2\, b_{SD})$. For $b_{SD} \cong 10\ (\text{GeV}/c)^{-2}$, which is the diffractive slope expected at the SPS Collider if $b_{SD}/b_{e\ell} = 2/3$, the value of η at the maximum of the distribution is $\cong 1.1$. This value is not very sensitive to the value of s, since b_{SD} is expected to increase only logarithmically with s.

Figure 13 shows the distribution predicted by Eq. (15) for the SPS Collider. In deriving Eq. (15), the width of the charged multiplicity distribution was neglected. At each mass M_x the multiplicity was taken to be the average value, $\bar{n}_c = 2\, M_x^{1/2}$. Had we taken the multiplicity width into account, the solid curve in Figure 13 would have been somewhat broader.

The dissociation of the "other" particle results in a curve identical to that shown in Figure 13 but at negative values of pseudo-rapidity. Double diffraction dissociation events are expected to have pseudo-rapidity distributions similar to that of Figure 13 but extending to both positive and negative values of η.

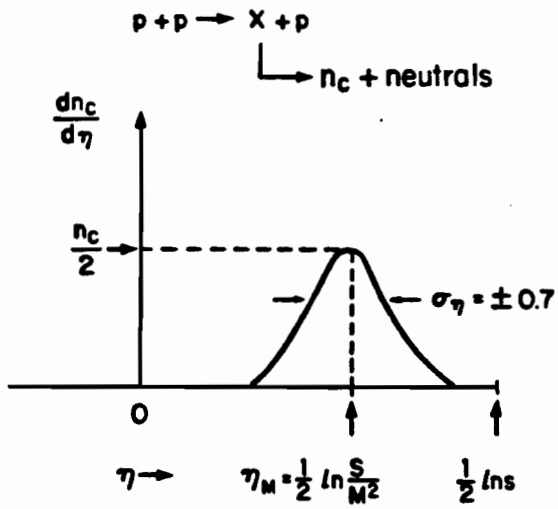

Fig. 9. Pseudo-rapidity distribution of charged particles from an isotropic decay of a diffractive state X of mass M for pp → Xp at (c.m.energy)^2=s.

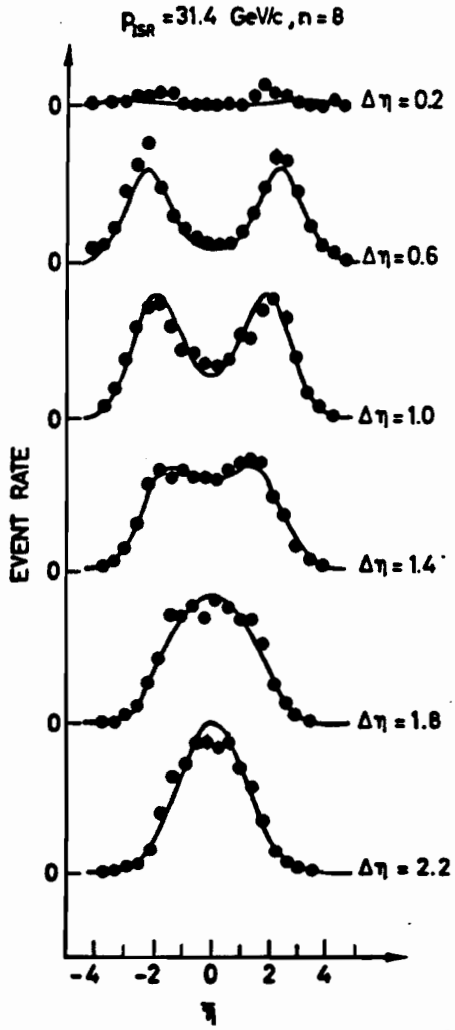

Fig. 10. Distributions of the mean pseudo-rapidity $\bar{\eta}$ for events with a given $\Delta\eta$ and fixed charged multiplicity from pp collisions at p_{ISR} = 31.4 GeV/c at the ISR [Ref. 8].

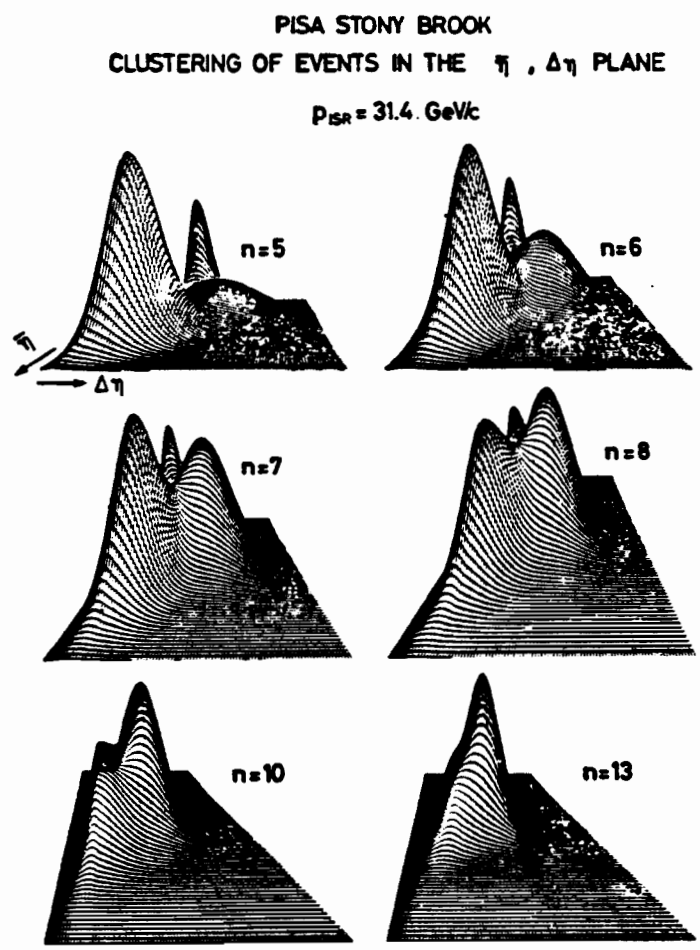

Fig. 11. The mean pseudo-rapidity $\bar{\eta}$ versus the width $\Delta\eta$ at various charged multiplicities for events from pp collisions at p_{ISR} = 31.4 GeV/c at the ISR [Ref. 8].

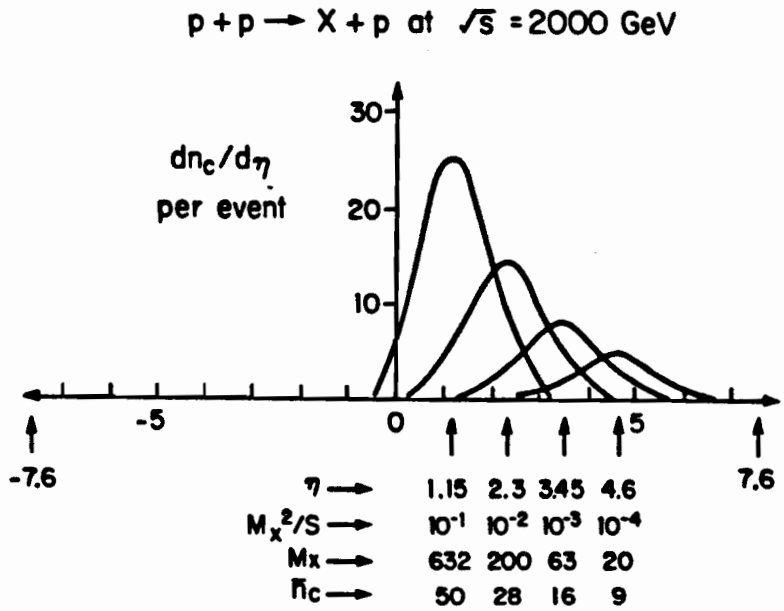

Fig. 12. Pseudo-rapidity distributions of charged particles from isotropic decays of diffractive states expected for pp → Xp at $\sqrt{s}$ = 2000 GeV (Fermilab Collider). The average charged multiplicity of a diffractive mass M_x is assumed to be $\bar{n}_c = 2M_x^{\frac{1}{2}}$

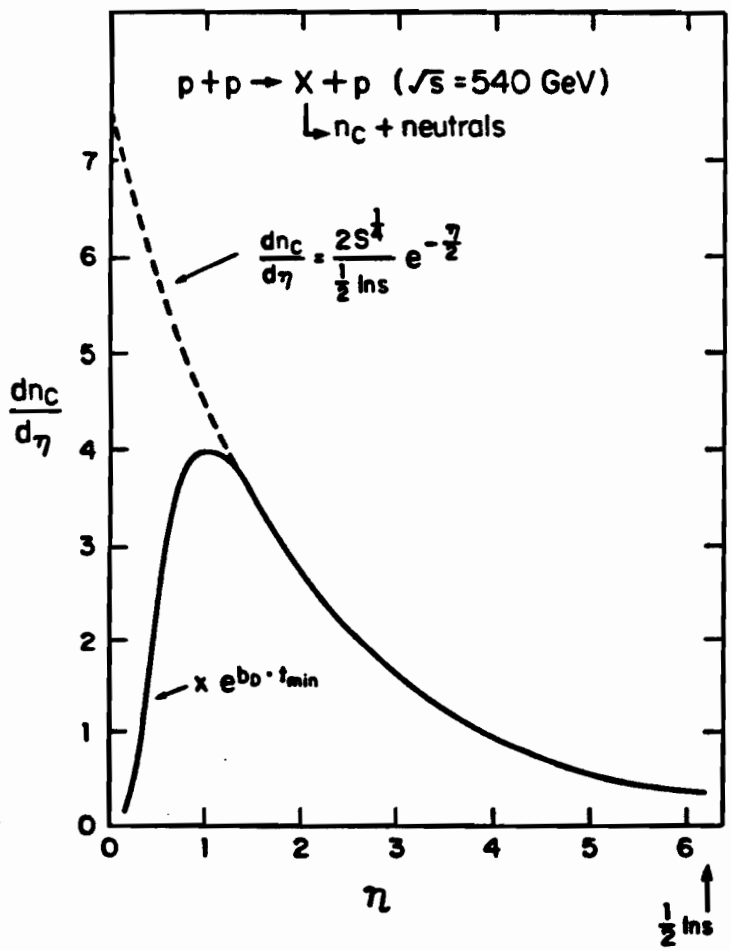

Fig. 13. Pseudo-rapidity distribution expected for single diffraction dissociation events, pp → Xp, at $\sqrt{s}$ = 540 GeV (SPS Collider). It is assumed that $d\sigma/dM_x^2 \sim 1/M_x^2$ and $\bar{n}_c = 2\,M_x^{\frac{1}{2}}$.

REFERENCES

1. K. Goulianos, Diffractive Interactions of Hadrons at High Energies, Rockefeller University Report No. RU 81/A-23, submitted to the XXI Intl. Conference on High Energy Physics, Paris, France (July 1982).
2. K. Goulianos, Slope of pp Elastic Scattering at Small Momentum Transfer, Phys. Rev. D24:26 (1981).
3. Alan R. White, Diffraction in Accelerators, Colliders and QCD, AIP Conf. Proc. No 85 - Proton-Antiproton Collider Physics - 1981 - V. Barger, D. Cline, F. Halzen (Eds.), Madison, Wisconsin (American Institute of Physics, New York, 1982), pp. 363-434.
4. T.J. Chapin, R.L. Cool, K. Goulianos, K.A. Jenkins, H. Sticker and S.N. White, Rockefeller University, "A Proposal to Measure Single and Double Diffraction Dissociation at the Fermilab $\bar{p}p$ Collider," (submitted to Fermilab October 1982).
5. R.L. Cool, K. Goulianos, S.L. Segler, H. Sticker and S.N. White, Charged Multiplicities of High Mass Diffractive $\pi^{\pm}$, $K^{\pm}$ and $p^{\pm}$ States, Phys. Rev. Lett. 48:451 (1982).
6. K. Goulianos, Universality of Charged Multiplicity Distributions, AIP Conf. Proc. No. 85 - Proton-Antiproton Collider Physics - 1981 - V. Barger, D. Cline, F. Halzen (Eds.), Madison, Wisconsin (American Institute of Physics, New York, 1982), pp. 469-485.
7. K. Goulianos, H. Sticker and S.N. White, Universality of Charged Multiplicity Distributions, Phys. Rev. Lett. 48:1454 (1982).
8. G. Belletini, AIP Conf. Proc. No. 15 - High Energy Collisions - 1973 (Stony Brook), Chris Quigg (ed.), (American Institute of Physics, New York, 1973), pp. 9-46.